# Adventures in Crystal Engineering

## Edward RT Tiekink

## Abstract

Crystals are all around us and are aesthetically pleasing as they arise from the ordered, three-dimensional assembly of chemical species which can be minerals (e.g. salt), macromolecules (e.g. proteins) or smaller chemical species (e.g. drugs, natural products, coordination complexes, etc.). Scientists need to know the precise structure of all these materials in order to rationalise the way they work. To put it in another way, "structure determines function". Single-crystal X-ray crystallography is the crucial technique behind the determination of crystal structure. Despite the prevalence and obvious importance of crystals, what remains an enormous challenge in contemporary science is to answer the fundamental question of "How do crystals form?". The goal of crystal engineering is to control the way molecules self-assemble in the condensed phase and the present discussion relates to this topic, an on-going research programme undertaken at Sunway University.

## Introduction

X-ray diffraction experiments on single crystals have played a pivotal role in providing the scientific community precise structural information at atomic resolution. A convenient way of comprehending the importance of X-ray crystallography upon the advancement of science is to consider the 29 Nobel Prizes awarded to almost 50 laureates employing X-ray crystallography in their research (International Union of Crystallography, n.d.). Indeed, the first Nobel Prize in Physics was awarded to Wilhelm C Röntgen for the *Discovery of X-rays* in 1901. Subsequent awardees were also drawn from the discipline of Physics, although mainly from Chemistry with some from Physiology or Medicine. Single-crystal X-ray crystallography stands alone in revealing the positions of electrons in crystals and, by implication, the location of nuclei in crystalline samples such as minerals, macromolecules and molecular chemistry. Examples of the types of structures that can be determined by crystallography are illustrated in Figure 1. The chosen example of a mineral structure is that of table salt, NaCl. As illustrated in Figure 1(a), the structure can be described as sodium cations ($Na^+$) surrounded by six chloride anions ($Cl^-$) that define an octahedron, i.e. a cubic close packed array of $Cl^-$ anions with $Na^+$ cations occupying all of the octahedral interstitial sites. This arrangement optimises attractive (electrostatic) interactions between oppositely charged species and, at the same time, minimises repulsions between like-charged species. In 2009, the Nobel Prize in Chemistry was awarded to Venkatraman Ramakrishnan, Thomas A Steitz and Ada E Yonath for their structural studies leading to the high-resolution structure determination of ribosome, an example of a macromolecular structure [Figure 1(b)] (Nobel Prize, n.d.). The example chosen for a molecular structure is that of another familiar

molecule, sucrose (sugar), as represented in Figure 1(c). This example is a perfect indicator of what information can be derived from an X-ray experiment, namely, bond lengths between atoms, bond, torsion and dihedral angles, relative conformations, absolute configuration, etc., all crucial in understanding the three-dimensional arrangement and, therefore, chemical behaviour.



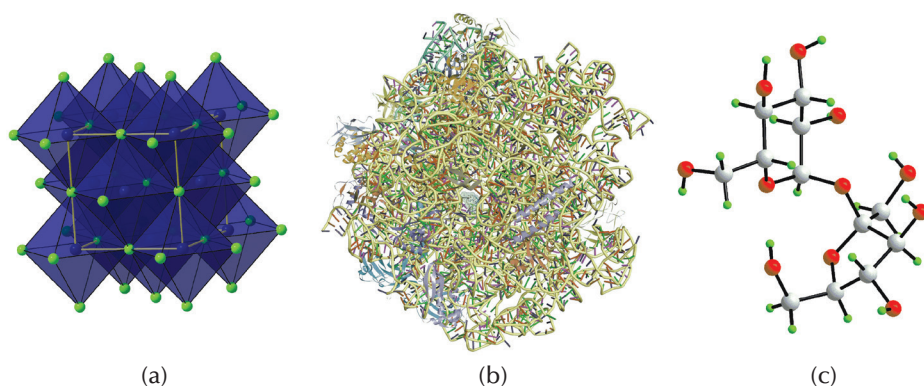(a)                              (b)                              (c)

FIGURE 1    Exemplars of structures determined by X-ray crystallography. (a) The extended, three-dimensional structure of NaCl (halite) representing minerals; blue and green spheres represent Na⁺ and Cl⁻ ions, respectively. (b) The structure of ribosome, an example of a macromolecular structure [Diagram courtesy of Professor Ignez Caracelli, Universidade Federal de São Carlos, and drawn with Biovia Discovery Studio 4.5 (Dassault Systemes Biovia, n.d.)]. (c) The molecular structure of sucrose, representing small molecules, which is the focus of this paper. Molecular structure diagrams are original and were generated with Diamond (Crystal Impact, n.d.). In (c), oxygen is represented by red spheres, carbon by grey and hydrogen by green spheres.

The foregoing paragraph clearly indicates how important X-ray crystallography has been and continues to be in the advancement of science. This is only possible because molecules, large and small, readily (by and large) crystallise to afford samples for analysis by crystallographers. However, there is a fundamental gap in our knowledge. Yes, crystals form and can be studied but, how do they form? To put it in another way, how do molecules self-assemble into

a regular arrangement to form crystals? In terms of frontier scientific endeavour, the question being pursued by crystal engineers is: given a specific molecule, can one control the way the molecules pack in the crystal? This desire has an analogy in synthetic chemistry in that the chemist works to form specific bonds between atoms to form molecules. On the other hand, the crystal engineer wishes to control the way molecules form their crystals. Well and truly beyond an intellectual pursuit, the control of the way individual molecules assemble implies control over a whole array of chemical and physical properties of crystalline materials, giving rise to new technology. In this paper, *Adventures in Crystal Engineering*, an account of the familiar and not-so-familiar is given, all revolving around the crucial issue: how do molecules form crystals?

## "Herding Cats"

There are several challenging obstacles to be overcome in order to design crystals, and several of these are discussed in this section. Firstly, it should be noted the following overview is confined to molecular compounds as opposed to minerals (comprising atoms/ions) and macromolecules, as these are normally very heavily solvated. The overarching principle underlying molecular packing, as mentioned earlier for the structure of NaCl, is that attractive interactions need to be maximised and, at the same time, repulsive interactions need to be minimised. Another principle is that free space in the crystal must be kept to a minimum as nature abhors a vacuum, *horror vacui*. This point is readily illustrated by a two-dimensional analogy. Consider a collection of squares and stack them vertically and horizontally. Immediately evident is that there is no free space between the square objects. The same happens when the shapes are triangular, rectangular and hexagonal. However, the

situation changes for pentagonal shapes. While there will be some edge-shared connections, free space is always apparent and hence, five-fold symmetry is precluded in the solid state. We need to be careful here, as five-fold symmetry can in fact be found in the solid state, as famously demonstrated by Daniel Shechtman, the Nobel Laureate in Chemistry in 2011. Five-fold objects are well-known in nature; just think of some starfish, many flowers and the next time you are eating a lady's finger (okra), but the suggestion that five-fold symmetry could exist in crystals attracted significant controversies (Lannin & Ek, 2011). Shechtman recognised localised regions of five-fold symmetry in studies of quasi-periodic crystals. This notwithstanding, avoiding free-space is a prerequisite of a stable three-dimensional arrangement of molecules. The next consideration is of the actual forces of attraction between molecules, commonly referred to as *inter*molecular interactions between molecules as opposed to *intra*molecular interactions found within molecules.

## Hydrogen-bonding

A number of specific intermolecular interactions are known to exist between molecules, and not just in the solid state. The most widely known of these are hydrogen-bonds. Referring to Figure 2, these are electrostatic interactions whereby an electron-deficient hydrogen atom, indicated by $\delta^+$ and which arises largely due to significant
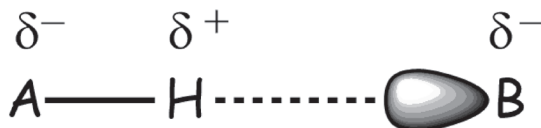


FIGURE 2    A schematic diagram showing the essential features of a hydrogen-bond (dashed line) formed between electron-deficient hydrogen and an electron-rich species, often a lone-pair of electrons.

polarisation in the A–H bond, is attracted to electron-rich donor atom, B; atoms A and B are considered electronegative. Hydrogen, being small, can approach B at quite close distances, consistent with hydrogen-bonds being directional and strong.

It is hydrogen-bonding that explains why ice floats on water — the hydrogen-bonds keep the molecules, relatively, further apart in ice and hence, the density is lower than that of water. Indeed, hydrogen-bonding has been employed extensively in the crystal engineering community. As seen in Figure 3, individual sucrose molecules [Figure 1(c)] are connected into a three-dimensional crystal by an extensive
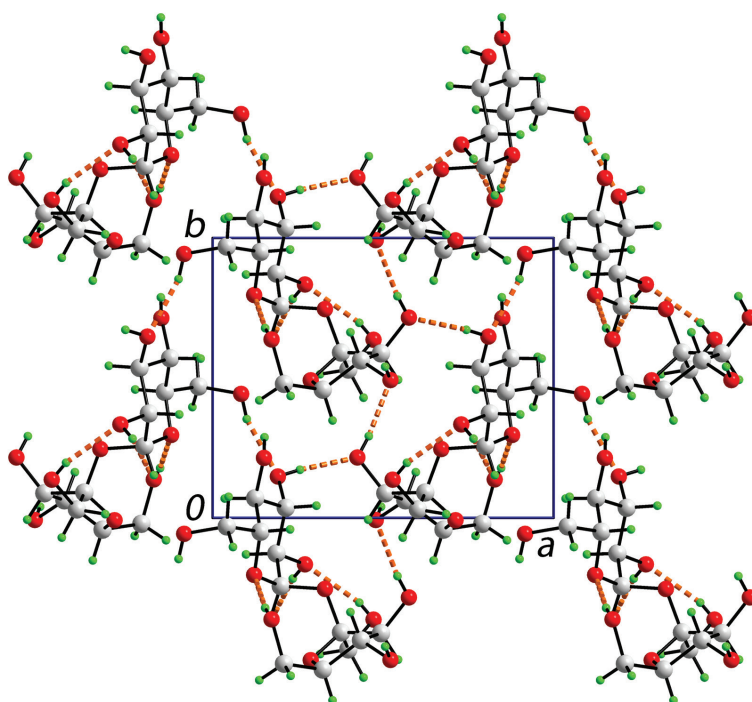


FIGURE 3 Molecular packing in a crystal of sucrose. A view of the unit cell contents down the c-axis showing hydrogen-bonding interactions between sucrose molecules as orange dashed lines.

array of hydrogen-bonding interactions between hydroxyl groups. Despite hydrogen-bonding having the attributes of being strong and directional, one cannot be absolutely certain that the desired hydrogen-bonds will occur in a crystal. This is because intermolecular interactions such as these are intrinsically weaker than comparable covalent bonds, being usually less than 10% the strength. Also, there can be competing intermolecular interactions at play, as will be discussed shortly. The problem with the inherently weak nature of hydrogen-bonding (and other intermolecular interactions) is seen in the phenomenon of polymorphism.

In crystallography, polymorphism refers to the situation where the same molecule (same connectivity, bonds, conformation, etc.) crystallises with different symmetry, e.g. a different pattern of hydrogen-bonding (or other intermolecular interactions). This is of fundamental importance, for example, to the pharmaceutical industry where, potentially, different polymorphs can lead to distinct Intellectual Property (IP) claims with substantial impact on revenue (Almarsson & Zaworotko, 2004). The enormity of the tasks facing crystal engineers is the observation that the lattice energy of polymorphs can differ by only a few kcal/mol — how can one impose a specific pattern upon molecules when the energy differences calculated for 10s up to 100 permutations of packing arrangements can differ by such a small energy (Price, 2014)? In fact, the desire to minimise the propensity of drugs to crystallise in different polymorphs gave rise to an important branch of crystal engineering, namely pharmaceutical co-crystals. Briefly, non-derivatisation of Active Pharmaceutical Ingredients (APIs), i.e. drugs, is accomplished by co-crystallising an API with another species that is usually associated with the drug via hydrogen-bonding. The co-crystal coformer is often drawn from a list of

Generally Regarded As Safe (GRAS) compounds that are safe/non-toxic, and in favourable circumstances, the new species will have better properties than the original drug, e.g. solubility, shelf-life, etc., and, therefore, is patentable (Bolla & Nangia, 2016). In essence, this branch of crystal engineering is designed to deliver a drug to a patient in a more effective/efficient manner and therefore attracts considerable interest in the pharmaceutical industry. From the perspective of the present discussion, it is the utilisation of strong hydrogen-bonding leading to new species that is relevant and points to the reliability of hydrogen-bonding in crystals. Designed hydrogen-bonding can also be exploited in another area of crystal engineering, namely to facilitate solid-state reactions.

Referring to Figure 4, two molecules can be deliberately held in positions to enable a solid-state reaction. In the illustrated example, two bipyridyl molecules, with the pyridyl rings separated by chains substituted with two C=C double bonds, are held in place by four, strong hydroxyl-O–H···N(pyridyl) hydrogen-bonds. Upon irradiation with UV-radiation, a sequence of [2+2] cycloadditions occurs between two pairs of C=C bonds in the chains, giving rise to a "ladderane", a molecule with the appearance of a ladder, albeit a little dilapidated (Gao, Friščić, & MacGillivray, 2004). This is a triumph of crystal engineering as conventional synthetic chemistry struggles to form such species, whereas the new technology enables their efficient synthesis in up to 100% yield.

The other point that needs to be emphasised here is that there is a considerable movement of atoms in these solid-state reactions and yet the crystals remain intact — the solid-state environment does not imply that motion is impossible.
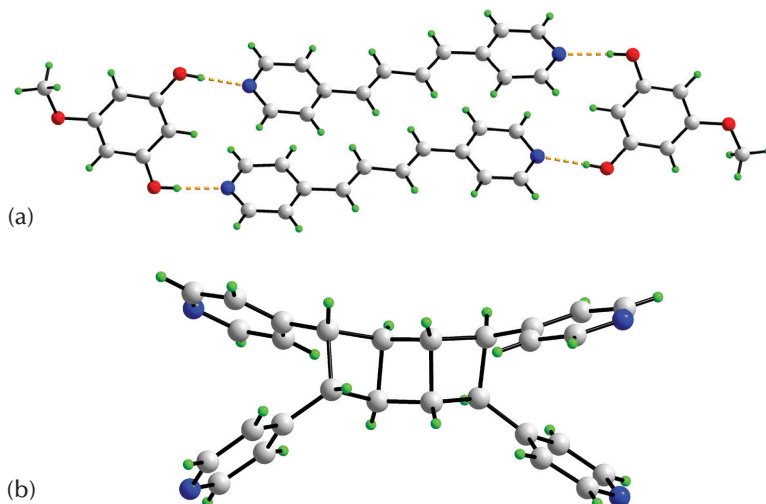
(a)

(b)

Figure 4   The facile synthesis of a ladderane employing crystal engineering technology. (a) Two precursor molecules are held in position by hydroxyl-O–H⋯N(pyridyl) hydrogen-bonds shown as orange dashed lines. Upon the application of UV-radiation upon the crystal, a sequence of reactions between proximate C=C bonds occurs. Recrystallisation of the product yields ladderanes as shown in (b). Additional colour code: blue for nitrogen.

As indicated earlier, other intermolecular interactions occur in crystals, over and beyond hydrogen-bonding. In the next section, halogen-bonding will be shown to be at least competitive with hydrogen-bonding and this will lead to a discussion of other intermolecular interactions at play in crystals.

## Halogen-bonding

The concept of co-crystal formation was mentioned earlier in the context of generating better drugs.  Here, two types of co-crystal will be discussed; one stabilised by hydrogen-bonding and the other by halogen-bonding (Corradi, Meille, Messina, Metrangolo, & Resnati, 2000). Figure 5 shows an outline of the experiments to be described.
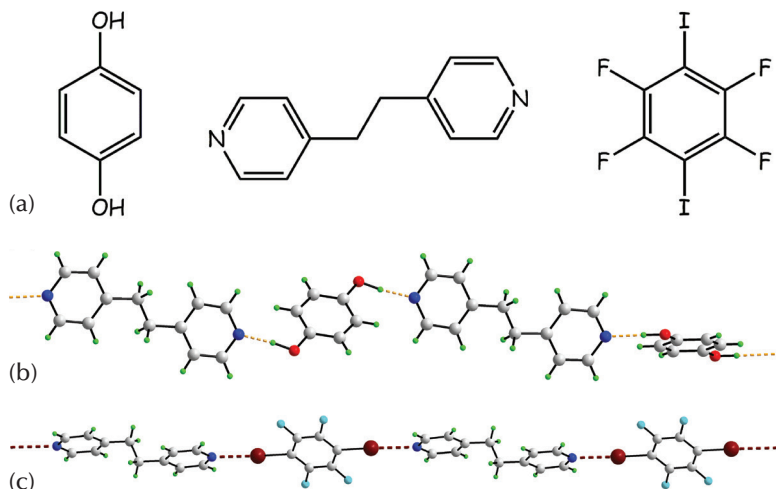
FIGURE 5 Crystallisation outcomes when the bipyridyl, di-hydroxyl and di-iodo-substituted molecules in (a) are co-crystallised in different experiments but under similar conditions. (b) The supramolecular polymer resulting from hydroxyl-O–H⋯N(pyridyl) hydrogen-bonding (orange dashed lines) after the 1:1 co-crystallisation of the bipyridyl and di-hydroxyl species. (c) The supramolecular polymer resulting from iodide⋯nitrogen halogen-bonding (brown dashed lines) after the 1:1 co-crystallisation of the bipyridyl and di-iodo species. Additional colour code: dark-red for iodide.

In Figure 5(a), three relevant molecules are illustrated. In the centre is the common molecule for each experiment, namely a bipyridyl derivative. On the left is a molecule capable of hydrogen-bonding through each of the hydroxyl groups (1,4-dihydroxybenzene) and, on the right, a molecule that can form halogen-bonding interactions through the iodide atoms (1,4-di-iodotetrafluorobenzene). In the first experiment, equimolar amounts of the di-hydroxyl and bipyridyl species are added together in an acetone solution. It would be anticipated that a polymeric aggregation pattern is observed in the solid state owing to the presence of hydroxyl-O–H⋯N(pyridyl) hydrogen-bonding. As shown in Figure 5(b), this, in fact, occurs. In the next experiment, equimolar quantities of the di-iodo

and bipyridyl species are added together in the same solvent. A supramolecular polymer again results, as illustrated in Figure 5(c). The next experiment is designed as a competition experiment. Here, molar equivalents of the di-hydroxyl and di-iodo species are added to one molar equivalent of the bipyridyl molecule. What results in the crystals that form? Before the answer is given to this question, we will consider the nature of the supramolecular interactions occurring between the iodide and nitrogen atoms shown in Figure 5(c).

As mentioned earlier in the context of the description of the crystal structure of NaCl, oppositely-charged species are attracted to each other via electrostatic interactions. What, then, is happening in the case of the structure shown in Figure 5(c) where electron-rich iodide (with three lone-pairs of electrons) atoms are interacting with electron-rich nitrogen atoms (each with one lone-pair of electrons)? Surely, these should be repulsive rather than attractive. Computational chemistry provides the answer in terms of an anisotropic distribution of electron density about the iodide atom. Referring to Figure 6, which shows a part of the repeat unit in the supramolecular chain of Figure 5(c), the electron-rich regions about the iodide and nitrogen atoms are indicated by the $\delta^-$ symbols. The crucial point is that the electron-density about the iodide atom is uneven with a build-up of electron-density in the
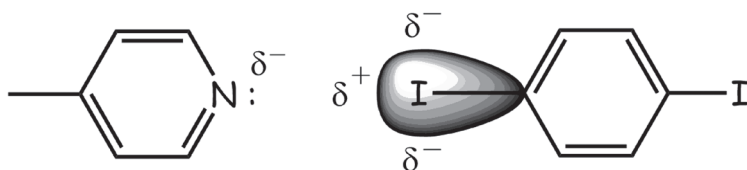


FIGURE 6   Proposed bonding interaction between electron-rich pyridyl-nitrogen and iodide atoms. The $\delta^+$ represents an electron-deficient region in the electron distribution about the iodide atom and this participates in an electrostatic interaction with the pyridyl-nitrogen atom.

region about and extending along the C–I bond but, at the tip of the latter, there is an electron-deficient region. This polar-cap or σ-hole is capable of accepting electron-density in the form of the lone-pair of electrons from the pyridyl-nitrogen to form a quite stable interaction. Despite the expectation of repulsive interactions between negatively charged entities, based on conventional thinking, halogen-bonding as exhibited between the pyridyl-nitrogen and iodide atoms in Figure 5(c) is attractive and can lead to well-defined supramolecular architectures.

So, what is the outcome of the experiment described earlier where all three species shown in Figure 5(a) are present in the same co-crystallisation experiment? The answer is that crystals of the supra-molecular polymer shown in Figure 5(c) are formed with evidence for the di-hydroxyl species remaining in solution. While different reasons based on solubility differences, kinetics, etc., might account for this experimental observation, this result indicates the fact that halogen-bonding is, at least, competitive with hydrogen-bonding.

It turns out that there is a myriad of other intermolecular interactions that can occur in crystals. These interactions become more and more important when either one or both hydrogen-bonding and halogen-bonding do not occur, or do occur only to give rise to zero-, one- or two-dimensional aggregation patterns. Examples of other widely recognised intermolecular interactions are those involving π-systems of the type π···π, O–H···π, C–H···π, etc., secondary bonding interactions between a main group element and an electron-rich system, typically a lone-pair of electrons, as well as some others to be described later. All of the aforementioned intermolecular interactions can potentially occur when crystals are

formed, and controlling which specific interaction will form is the challenge of crystal engineering, a task so far proving largely elusive and appearing to be akin to "herding cats".

## Size Does Matter

In this section, a description of a design element in crystal engineering is presented based on the steric bulk of organic substituents in ligands bound to metal centres. The concept is simple and basically states that if the size of a ligand-substituent around a metal centre is too big, molecules cannot approach each other to form secondary-bonding interactions and, therefore, supramolecular aggregation is "turned-off". In terms of crystal engineering, the following example of binary zinc xanthates, i.e. molecules of the general formula $Zn(S_2COR)_2$, R = Et, *n*-Pr and *i*-Pr (Figure 7), is a nice exemplar of the concept and a particular favourite of the author (Lai, Lim, Yap, & Tiekink, 2002).
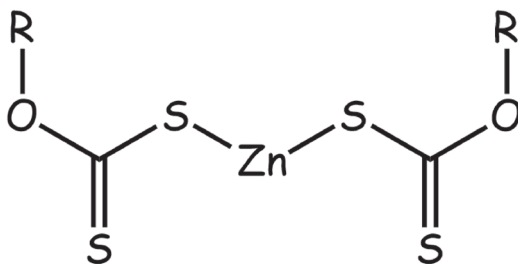


FIGURE 7    Generic chemical diagrams of $Zn(S_2COR)_2$ for R = Et, *n*-Pr and *i*-Pr. Each of these molecules self-associates in their respective crystal but each gives rise to a distinct aggregation pattern based on the size of R.

Referring to Figure 8, the molecular structure of $Zn(S_2CO\text{-}i\text{-}Pr)_2$ is an isolated tetramer comprising a square of four zinc atoms with each edge defined by a bidentate, bridging xanthate ligand. Each of

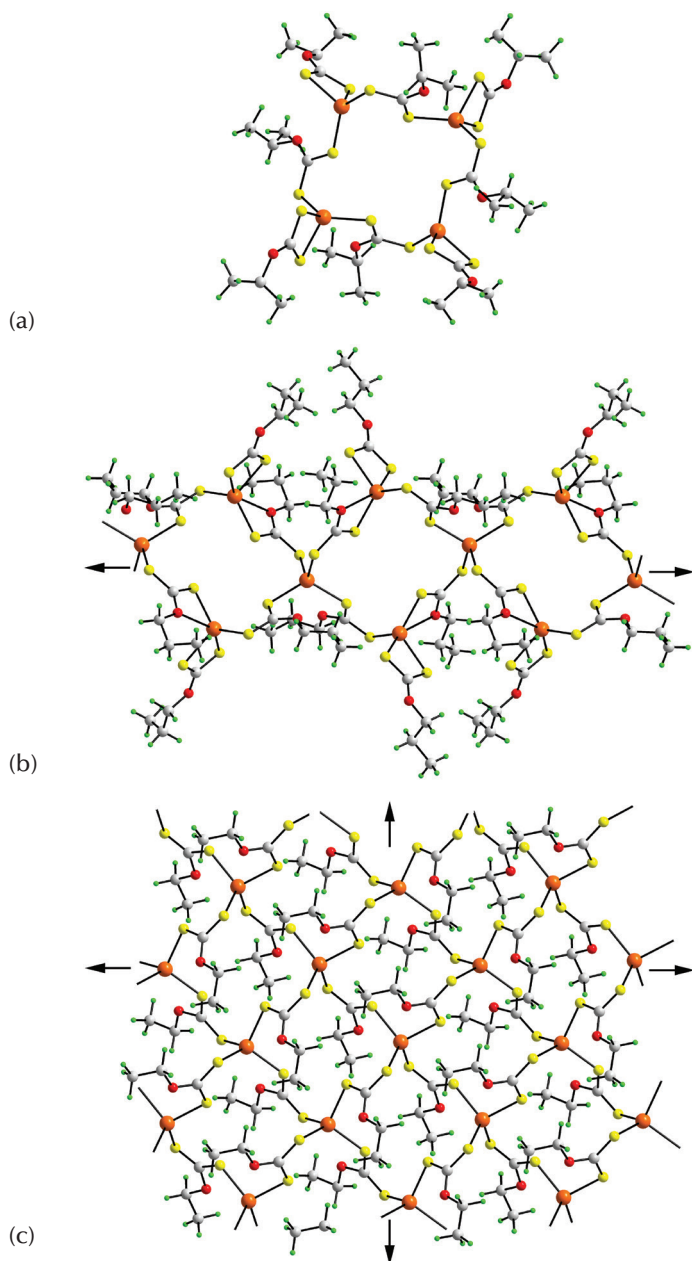FIGURE 8    Solid-state structures of $Zn(S_2COR)_2$. (a) An isolated tetramer for R = *i*-Pr. (b) A supramolecular chain for R = *n*-Pr. (c) A supramolecular layer for R = Et. Additional colour codes: orange for zinc (in subsequent diagrams, other heavy elements, i.e. cadmium, copper, arsenic and gold); yellow for sulphur.

the remaining four xanthate ligands chelates a zinc centre [Figure 8(a)]. When the steric bulk of the branched isopropyl group is reduced to the straight chain, i.e. *n*-propyl, a huge change in structure is observed. In the crystal of $Zn(S_2CO$-*n*-$Pr)_2$, shown in Figure 8(b), the tetramers of Figure 8(a) are retained but are now corner-shared, leading to a linear chain, as the ratio of bridging to chelating xanthate ligands has changed from 1:1 for $Zn(S_2CO$-*i*-$Pr)_2$ to 2:1 for $Zn(S_2CO$-$n$-$Pr)_2$. When the steric bulk of the R group is reduced even further, i.e. to ethyl, as in $Zn(S_2COEt)_2$, all of the xanthate ligands are now bridging as shown in Figure 8(c), with the result that the tetramers are edge-shared and assembled into a layer.

The engineering analogy for the three structures illustrated in Figure 8 relates to the basic repeat unit of the three structures, being the tetrameric unit, i.e. the paving stone [Figure 9(a)]. When the steric bulk of R is great, a three-dimensional exclusion zone is defined about the molecular paving stone. This happens in the case of large R groups such as *iso*-propyl, whereby no aggregation between paving stones is possible so that the paving stone is isolated [Figure 9(a)]. When the size of the R group is decreased to *n*-propyl, the hindrance is reduced so that the molecular paving stones can be corner-shared with the resultant change in architecture [Figure 9(b)]. Finally, when there is a minimal hindrance precluding connections between tetrameric units (the ethyl groups are directed occurring above and below the plane) as in the case of R = Et, the molecular paving stones can approach each other with no impediment to give a paved layer [Figure 9(c)].

(a)                                    (b)                                    (c)

FIGURE 9    Molecular paving with Zn(S$_2$COR)$_2$. (a) The basic repeat unit based on the isolated tetrameric unit found in Zn(S$_2$CO-*i*-Pr)$_2$. (b) The corner-shared paving stones found in the crystal of Zn(S$_2$CO-*n*-Pr)$_2$. (c) The layer of edge-shared paving stones found in the crystal of Zn(S$_2$COEt)$_2$.

## "Emerging" Supramolecular Interactions

In this section, several hitherto unrecognised intermolecular interactions are described. Of course, these have always existed in the relevant crystal structures but they have not been recognised previously as contributing to the stability of the molecular packing. Here, only single examples are given for each type of interaction as recent extensive literature surveys are available, as indicated.

As mentioned earlier, C–H···π interactions, where the π-system is an organic ring with delocalised electron density, are well-known to occur in crystals. Metal-complexes featuring chelating ligands can form analogous electron-rich rings, i.e. chelate rings, and these too can potentially accept C–H interactions. Most probably, the first time these interactions were specifically mentioned in the literature was for the structure of Cd(S$_2$COCH$_2$CH$_2$OMe)$_2$(2,2′-bipyridyl) (Chen, Lai, & Tiekink, 2003) [Figure 10(a)]. Here, methyl-bound C–H hydrogen atoms are directed towards the centre of the four-membered CdS$_2$C chelate rings to provide stability to the molecular packing and to sustain a supramolecular layer as shown

in Figure 10(b). Such C–H···(chelate ring) interactions are gaining more and more attention in the literature (Tiekink & Zukerman-Schpector, 2011).
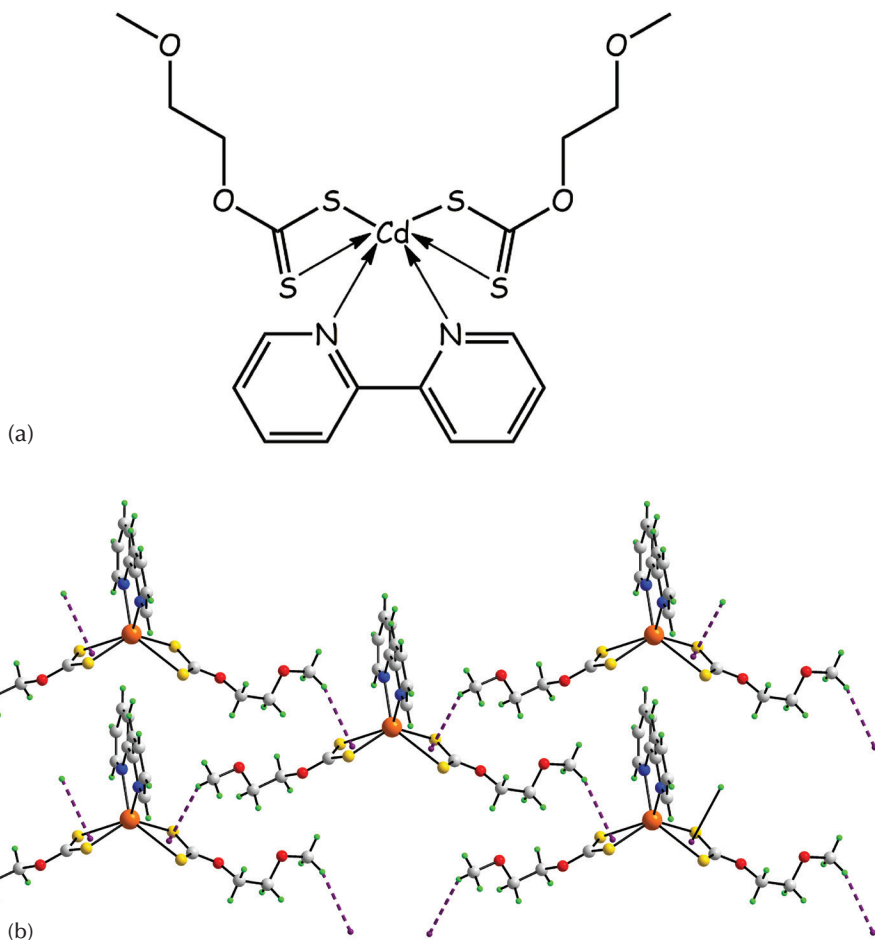


(a)

(b)

FIGURE 10 (a) Chemical diagram for Cd(S$_2$COCH$_2$CH$_2$OMe)$_2$(2,2′ -bipyridyl). (b) Molecular packing showing bipyridyl-C–H···π (CdS$_2$C) interactions as purple dashed lines.

Interactions between $\pi$-systems, i.e. $\pi{\cdots}\pi$ interactions, were also alluded to earlier. Often, these occur between organic ring systems but they can also occur between chelate rings, i.e. $\pi$(chelate ring)$\cdots\pi$(chelate ring) interactions. An example of such an interaction leading to a supramolecular chain is found in the structure of the square-planar copper(II) acetylacetonate complex shown in Figure 11(a). The aggregation between molecules in the crystal is shown in Figure 11(b), whereby supramolecular chains
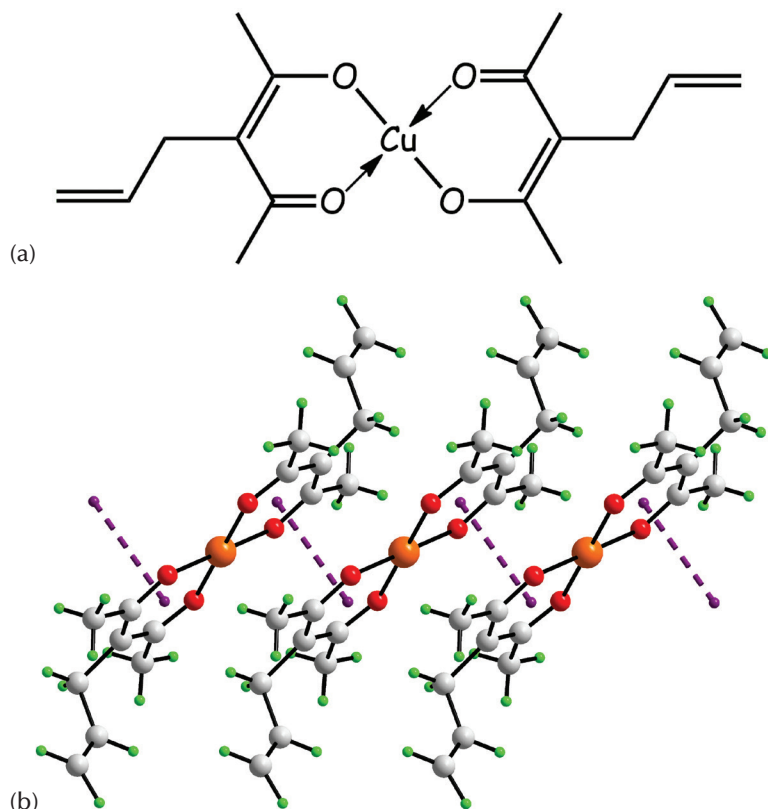


(a)



(b)

FIGURE 11   (a) Chemical diagram for bis(3-allylacetylacetonato)copper(II). (b) Molecular packing showing $\pi$(chelate ring)$\cdots\pi$(chelate ring) interactions as purple dashed lines, leading to a supramolecular chain in the crystal.

are sustained by π(chelate ring)⋯π(chelate ring) interactions. Highlighting the point made earlier, this structure was reported well over 30 years ago (Aruffo, Anderson, Lingafelter, & Schomaker, 1983) but it is only recently that the π⋯π interactions between chelate rings were described (Malenov, Janjić, Medaković, Hall, & Zarić, 2017).

Finally, the last "emerging" supramolecular interactions to be described here are the arsenic(lone-pair)⋯π interactions which exist in the structure of chlorido-(toluene-3,4-dithiolato)arsenic(III) [Figure 12(a)] (Kisenyi, Willey, Drew, & Wandiga, 2011); analogous interactions exist for all main group elements in low oxidation states (Caracelli, Haiduc, Zukerman-Schpector, & Tiekink, 2017). As suggested a few times earlier, one must look beyond conventional wisdom when discovering the way molecules assemble in crystals. Again, in the example shown in Figure 12(a), the situation arises when apparently two negatively-charged species face each other, yet the interaction between them is attractive. Theory comes to the rescue again in that the interaction in fact occurs between an electron-deficient region at the tip of the lone-pair of electrons on arsenic and the electron-cloud of the organic ring, akin to that described earlier for halogen bonding (Figure 7). The result of the arsenic(lone-pair)⋯π interaction is a supramolecular chain, as shown in Figure 12(b). Curiously and crucially, the structure also features chloride and sulphur atoms, yet there are no As⋯Cl or As⋯S interactions occurring in any dimension of the crystal. This suggests that the energy of stabilisation to the crystal afforded by the arsenic(lone-pair)⋯π interaction is of the same order of magnitude as the putative As⋯Cl and As⋯S interactions.
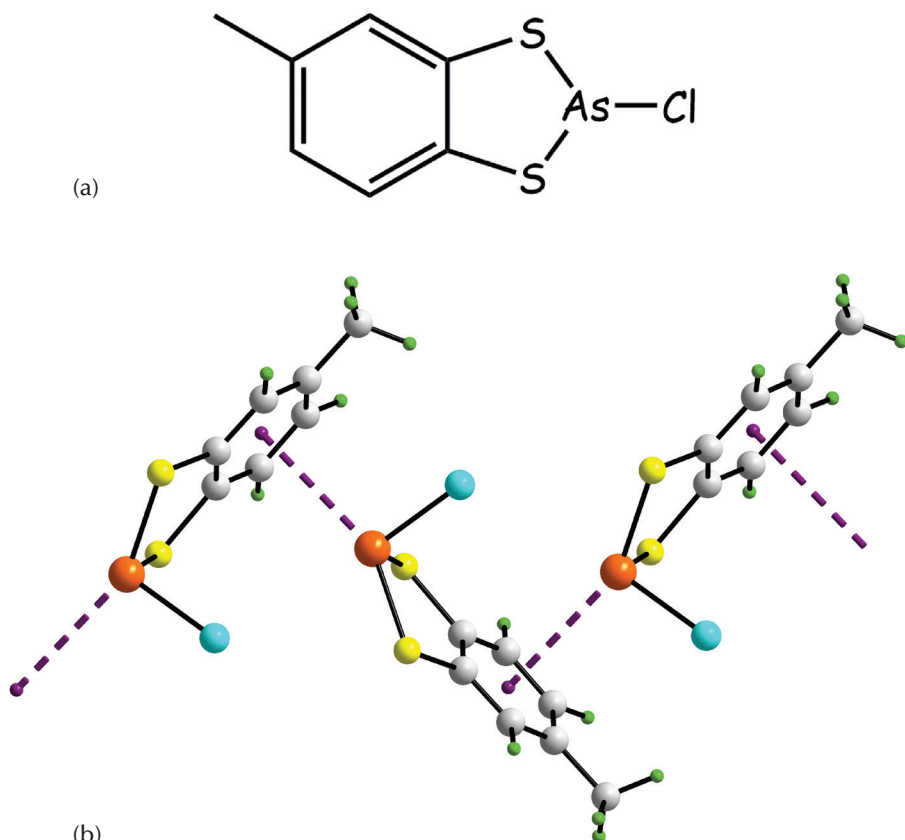
(a)



(b)

FIGURE 12 (a) Chemical diagram for chlorido-(toluene-3,4-dithiolato) arsenic(III). (b) Supramolecular chain in the crystal sustained by arsenic (lone-pair)···π interactions. Additional colour code: cyan for chloride.

## Global Crystal Packing

In this final section, two illustrative pairs of structures are discussed that point to another fundamental concept related to molecular packing (Tiekink, 2014; Tiekink, 2017). Thus far, the emphasis has largely been upon a supramolecular synthon approach (Desiraju, 1995) to visualise the way molecules assemble; in others words,

an approach based on specific interactions between molecules such as hydrogen-bonding. Here, molecules are envisaged to form interactions as they crystallise and thereby the supramolecular glue between molecules is the all-important determiner of the molecular self-assembly. At the other extreme, supramolecular synthons might be thought to arise as a result of the way molecules assemble, i.e. molecules crystallising and then forming supramolecular associations such as hydrogen-bonding (Dunitz & Gavezzotti, 2012; Gavezzotti, 2017). If global crystal packing is fundamental in the way molecules assemble, molecules should aspire to be spherical as the packing of spheres is the most efficient manner by which non-cubic (rectangular) objects can be assembled in a three-dimensional space. This assertion is supported experimentally in that in the overwhelming number of cases, molecules — which often have non-regular shapes — will crystallise about a centre of inversion, thereby attaining a more globular shape. In this section, two examples will be presented where conventional bonding interactions, either intramolecular or intermolecular, are seemingly usurped by the desire of the molecule in question to attain a spherical shape.

The first pair of structures to be described has the general formula $R_3PAu(S_2CO\text{-}c\text{-}C_6H_{11})$, where, as indicated by the green arrow in Figure 13(a), there is the possibility of unhindered rotation about the thiolate-S–C(quaternary) single bond. Before describing the two molecular structures of $R_3PAu(S_2CO\text{-}c\text{-}C_6H_{11})$, some fundamental chemistry needs to be mentioned. Under normal circumstances and conditions, two polarisable atoms will form an association in preference to an interaction involving polarisable/non-polarisable atoms. With this in mind, in the molecular structure shown in Figure 13(b), the gold atom exists in the expected linear geometry defined by the thiolate-S atom and phosphane-P atom. There is an

(a)

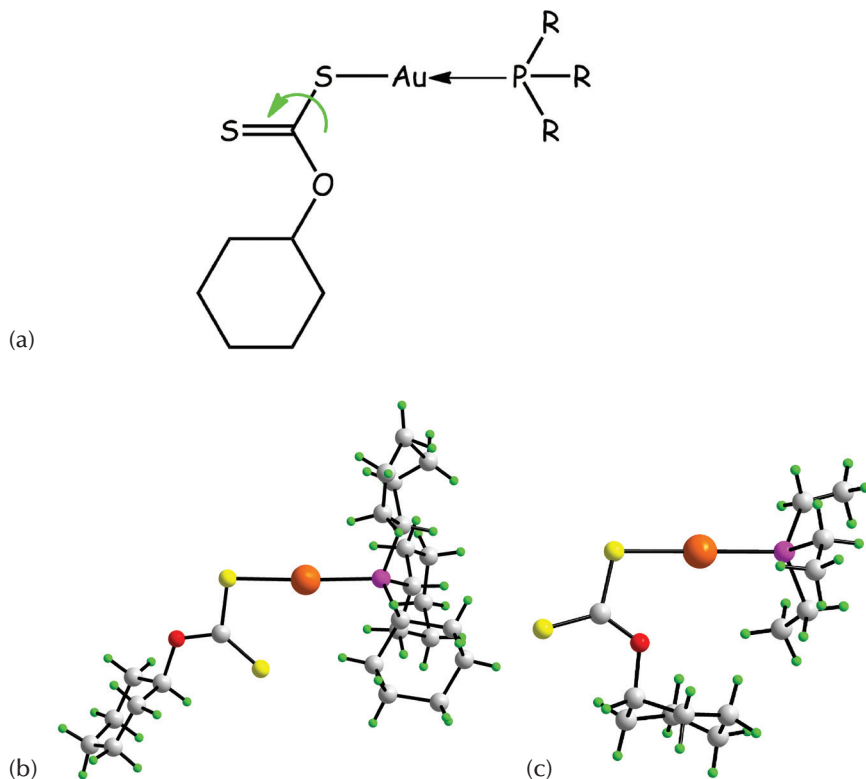(b)                                          (c)

FIGURE 13    (a) Generic chemical diagram for $R_3PAu(S_2CO-c-C_6H_{11})$.
(b) The anticipated S,S mode of coordination of the xanthate ligand.
(c) The unexpected S,O mode of coordination.
Additional colour code: pink for phosphorus.

intramolecular interaction that is formed between the gold atom and the non-coordinating-sulphur atom. Based on the paradigm just mentioned, this is expected as both gold and sulphur are considered polarisable, certainly when compared with oxygen. So, the molecular conformation shown in Figure 13(c) is, in fact, not expected, as an intramolecular Au···O interaction is formed instead of the expected Au···S interaction. Given that the phosphane ligands, i.e. R = cyclohexyl and ethyl in Figures 13(b) and (c) respectively, do

not exert a significant electronic influence upon the bonding, global crystal packing effects have been invoked for the explanation of the disparate conformations in these and related systems (Tiekink & Haiduc, 2005). Looking at the images in Figures 13(b) and (c), it is easy to note that on first inspection, the molecule in Figure 13(b) has an elongated structure, which might be termed a "rod". However, in the image shown in Figure 13(c), the form of the molecule is more spherical which might be termed a "ball". Given that spherical shapes give rise to more efficient packing (less free-space), the formation of a ball with an unfavourable intramolecular Au⋯O contact is promoted by the desire to attain more efficient molecular packing, i.e. global crystal packing considerations. The molecule in Figure 13(b) does not adopt a conformation with an intramolecular Au⋯O interaction owing to the ensuing steric hindrance between the bulky cyclohexyl substituents on both residues, in contrast to the small phosphorus-bound ethyl groups in the molecule in Figure 13(c).

Similar terminology and considerations apply to the two polymorphs of another phosphanegold(I) thiolate compound, namely, $(c\text{-}C_6H_{11})_3PAu(SC_6H_4\text{-}CO_2H\text{-}2)$ (Smyth, Vincent, & Tiekink, 2001) [Figure 14(a)]. In this molecule, free rotation is possible about the phenyl-C–C(carboxylic acid) bond and leads to different hydrogen-bonding patterns. Given smaller and more electronegative atoms, such as oxygen, are anticipated to form hydrogen-bonding interactions, certainly compared with sulphur, the supramolecular association via the cyclic eight-membered synthon $\{\cdots HOC=O\}_2$ is as expected [Figure 14(b)]. What was not expected was the appearance of another molecular conformation in a second polymorph, whereby an intramolecular hydroxyl-O–H⋯S(thiolate) hydrogen-bond was formed instead [Figure 14(c)]. Global crystal packing considerations come to the fore in this example as well. The molecule forming the
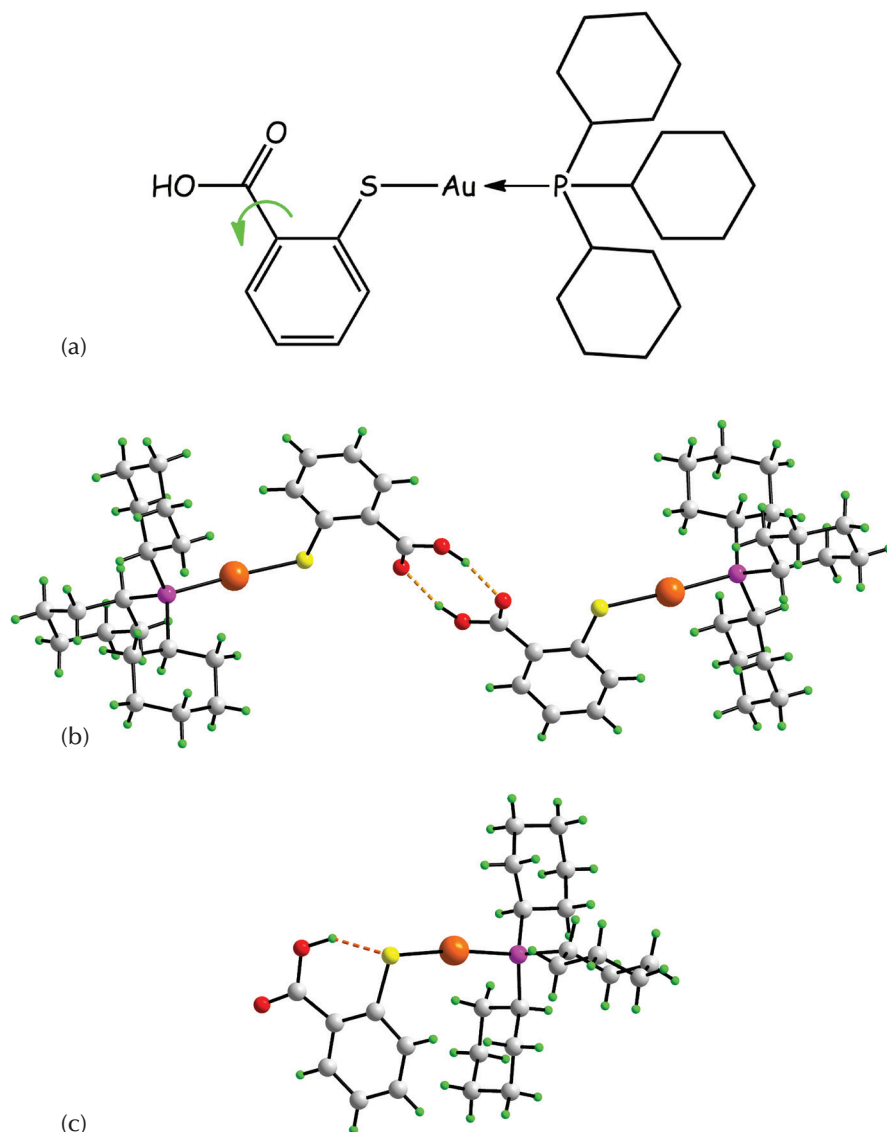
FIGURE 14 (a) Chemical diagram for ($c$-C$_6$H$_{11}$)$_3$PAu(SC$_6$H$_4$-CO$_2$H-2). (b) Supramolecular dimer sustained by intermolecular hydroxyl-O–H···O(carboxyl) hydrogen-bonding in the "rod" polymorph. (c) The molecular conformation sustained by an intramolecular hydroxyl-O–H···S(thiolate) hydrogen-bond in the "ball" polymorph.

expected hydrogen bonding pattern has a "rod" shape whereas that forming the unexpected intramolecular hydrogen bond has a "ball" shape. Thus, a competition between forming favourable hydrogen-bonding interactions and favourable shapes for molecular packing is at play. This is particularly so in the present case as both molecular conformations in their respective polymorphs crystallised from the same solution, i.e. an example of concomitant crystallisation, suggesting a fine balance in the energies of molecular conformation and molecular packing.

## Conclusion

The former editor of *Nature*, Sir John Maddox, described the inability of chemists/crystal engineers to design crystals of molecular compounds based on the knowledge of the molecular structure as a "scandal" (Maddox, 1988). That was back in 1988. While no doubt some important advances have been made since then, more progress is still needed for crystal engineering to be understood. Many of the examples cited earlier are actually instances of engineering within a crystal with the "design element" limited to forming zero- or one-dimensional aggregates within "uncontrolled" three-dimensional architectures. There are two key approaches proffered for the formation of crystals, either based on the supramolecular synthon concept, i.e. intermolecular forces dictate the way crystals form, or in terms of global crystal packing, i.e. molecules pack to optimise attractions, minimise repulsions and free-space, and the intermolecular contacts arise as a result of this optimisation. While it is likely that the principles governing molecular packing will contain elements of both, clearly, there is still much more to be done to delineate what exactly is going on when molecules assemble in crystals, and there are many more exciting discoveries to be made.

# References

Almarsson, Ö. & Zaworotko, M. J. (2004). Crystal engineering of the composition of pharmaceutical phases. Do pharmaceutical co-crystals represent a new path to improved medicines? *Chemical Communications*, 1888–1896. doi:10.1039/B402150A

Aruffo, A. A., Anderson, L. D., Lingafelter, E. C., & Schomaker, V. (1983). Bis(3-allylacetylacetonato)copper(II), $C_{16}H_{22}CuO_4$. *Acta Crystallographica*, *C39*, 201–203. doi:10.1107/S0108270183004114

Bolla, G. & Nangia, A. (2016). Pharmaceutical cocrystals: Walking the talk. *Chemical Communications*, *52*, 8342–8360. doi:10.1039/C6CC02943D

Crystal Impact. (n.d.) *Diamond: Crystal and molecular structure visualization.* Retrieved from http://www.crystalimpact.com/diamond

Caracelli, I., Haiduc, I., Zukerman-Schpector, J., & Tiekink, E. R. T. (2017). A new non-covalent bonding mode in supramolecular chemistry: Main group element lone-pair-π(arene) interactions. In D. W. Johnson & F. Hof (Eds.), *Aromatic interactions: Frontiers in knowledge and application (Monographs in supramolecular chemistry)* (pp. 98–123). London, UK: The Royal Society of Chemistry.

Chen, D., Lai, C. S., & Tiekink, E. R. T. (2003). Crystal structures of 2,2′-bipyridine adducts of two cadmium O-alkyl dithiocarbonates: Rationalisation of disparate coordination geometries based on different crystal packing environments. *Zeitschrift für Kristallographie*, *218*, 747–752. doi:10.1524/zkri.218.11.747.20300

Corradi, E., Meille, S.V., Messina, M. T., Metrangolo, P., & Resnati, G. (2000). Halogen bonding versus hydrogen bonding in driving self-assembly processes. *Angewandte Chemie International Edition*, *39*, 1782–1786. doi:10.1002/(SICI)1521-3773(20000515)39:10<1782::AID-ANIE1782>3.0.CO;2-5

Desiraju, G. R. (1995). Supramolecular synthons in crystal engineering—A new organic synthesis. *Angewandte Chemie International Edition*, *34*, 2311–2327. doi:10.1002/anie.199523111

Dassault Systemes Biovia. (n.d.). *Visualization: Biovia discovery studio*. Retrieved from http://accelrys.com/products/collaborative-science/biovia-discovery-studio/visualization.html

Dunitz, J. D. & Gavezzotti, A. (2012). Supramolecular synthons: Validation and ranking of intermolecular interaction energies. *Crystal Growth & Design, 12*, 5873–5887. doi:10.1021/cg301293r

Gao, X., Friščić, T., & MacGillivray, L. R. (2004). Supramolecular construction of molecular ladders in the solid state. *Angewandte Chemie International Edition*, *43*, 232–326. doi:10.1002/anie.200352713

Gavezzotti, A. (2017). Topics in structural chemistry through after-dinner humor. *Israel Journal of Chemistry*, *57*, 13–23. doi:10.1002/ijch.201600024

International Union of Crystallography. (n.d.). *Nobel Prize winners associated with crystallography*. Retrieved from https://www.iucr.org/people/nobel-prize

Kisenyi, J. M., Willey, G. R., Drew, M. G. B., & Wandiga, S. O. (2011). Toluene-3,4-dithiol ($H_2$tdt) complexes of group 5B halides. Observations of lone-pair stereochemical activity and redox behaviour. Crystal and molecular structures of [AsCl(tdt)] and [$PPh_4$][Sb(tdt)$_3$]. *Journal of the Chemical Society*, *Dalton Transactions*, 69–74. doi: 10.1039/DT9850000069

Lai, C. S., Lim, Y. X., Yap, T. C., & Tiekink, E. R. T. (2002). Molecular paving with zinc thiolates. *CrystEngComm*, *4*, 596–600. doi:10.1039/B210187D

Lannin, P. & Ek, V. (2011, October 5). Ridiculed crystal work wins Nobel for Israeli. *Reuters*. Retrieved from https://www.reuters.com/article/nobel-chemistry-idUSL5E7L51U620111005

Maddox, J. (1988). Crystals from first principles. *Nature*, *335*, 201. doi:10.1038/335201a0

Malenov, D. P., Janjić, G. V., Medaković, V. B., Hall, M. B., & Zarić, S. D. (2017). Noncovalent bonding: Stacking interactions of chelate rings of transition metal complexes. *Coordination Chemistry Reviews*, *345*, 318–341. doi:10.1016/j.ccr.2016.12.020

Nobel Prize. (n.d.). *Nobel prizes and laureates.* Retrieved from https://www.nobelprize.org/nobel_prizes/chemistry/laureates/2009/illpres.html

Price, S. L. (2014). Predicting crystal structures of organic compounds. *Chemical Society Reviews*, *43*, 2098–2111. doi:10.1039/c3cs60279f

Smyth, D. R., Vincent, B. R., & Tiekink, E. R. T. (2001). Polymorphism in (tricyclohexylphosphine)gold(I) 2-mercaptobenzoate — A tale of two structural motifs. *Crystal Growth & Design*, *1*, 113–117. doi:10.1021/cg0000114

Tiekink, E. R. T. (2014). Molecular crystals by design? *Chemical Communications*, *50*, 11079–11082. doi:10.1039/C4CC04972A

Tiekink, E. R. T. (2017). Supramolecular assembly based on "emerging" intermolecular interactions of particular interest to coordination chemists. *Coordination Chemistry Reviews*, *345*, 209–228. doi: doi.org/10.1016/j.ccr.2017.01.009

Tiekink, E. R. T. & Haiduc, I. (2005). Stereochemical aspects of metal xanthate complexes: Molecular structures and supramolecular self-assembly. *Progress in Inorganic Chemistry*, *54*, 127–319. doi: 10.1002/0471725560.ch

Tiekink, E. R. T. & Zukerman-Schpector, J. (2011). Emerging supramolecular synthons: C–H⋯π (chelate) interactions in metal bis(1,1-dithiolates). *Chemical Communications*, *47*, 6623–6625. doi:10.1039/C1CC11173F

# About the Author



**Edward RT Tiekink** is a graduate of University of Melbourne, achieving a First Class Honours degree (1981), a PhD in Inorganic Chemistry (1985) and a DSc (2006). After a postdoctoral appointment in molecular crystallography at University of Adelaide, he joined the academic staff there in 1989. Since 2001, Professor Tiekink has held several overseas appointments before joining Sunway University in November 2015. As Distinguished Professor at Sunway University and Head of the Research Centre for Crystalline Materials, Professor Tiekink is establishing new research directions in the general area of molecular crystallography and metal-based drugs.